Applied Soft Computing 70 (2018) 169–181

Contents lists available at ScienceDirect

Applied Soft Computing

journal homepage: www.elsevier.com/locate/asoc

Multi-objective transmission congestion management considering demand response programs and generation rescheduling

Fariborz Zaeim-Kohan, Hadi Razmi*, Hasan Doagou-Mojarrad

Department of Electrical Engineering, East Tehran Branch, Islamic Azad University, Tehran, Iran

ARTICLE INFO

Article history:
Received 4 July 2017
Received in revised form 25 March 2018
Accepted 16 May 2018
Available online 21 May 2018

Keywords:
Transmission congestion management
Demand response programs (DRPs)
Generation rescheduling
Multi-objective particle swarm optimization (MOPSO)

ABSTRACT

With the implementation of restructuring and deregulation in the electricity industry, efficient and economic operations of power systems have become remarkably significant. Meanwhile, congestion in transmission lines is one of the major problems in power system operation. Therefore, in this paper, the multi-objective particle swarm optimization (MOPSO) method has been used for transmission congestion management considering demand response programs (DRPs) and generation rescheduling. Total operation/DR cost, emission and increasing the loading of transmission lines are the objective functions of this problem. Using DRPs increases the operator power of choice with regard to the participation of small consumers in reducing the demand. The method already mentioned has been tested on two test systems (IEEE 30-bus and IEEE 118-bus test systems). The results of the evaluation in the form of different scenarios show that DRPs reduce the power system transmission lines congestion, allowing the use of the transmission lines with less loading capacity. Also, in some instances, without using DRPs, solving the transmission congestion management problem is impossible.

1. Introduction

With restructuring and increasing demand, utilizing the maximum capacity of transmission lines becomes more important. In this way, transmission lines congestion increases subsequently resulting in reduced margin of system security and stability, electrical power outages, damage to equipment, and the lack of proper implementation of the electricity market contracts [1].

Measures taken to eliminate or improve the congestion are called congestion management. Congestion management allows market operators to have the maximum use of the network, and maintain the security of the system. Thus, congestion management improves competition in all sectors of the electricity market [2].

Moreover, in vertical integrated traditional power system, the system operator determines the transmission line flows within the allowable range in the lowest cost. This is while in restructured power systems congestion management has become a bit complicated by separating generation, transmission, distribution and open access to the transmission network [3]. The solution in this case seems to be the construction of new transmission lines. However, some fundamental problems and barriers such as environmental restrictions, transmission right of way, and economic issues have made this idea impractical.

Nodal pricing method is one of the earliest methods of transmission congestion management [4]. With this pricing method, the independent system operator (ISO) is able to inject electricity at one point and receives electricity from another point to fix congestion. In [5], using nodal pricing, a new control scheme, is proposed to manage transmission lines congestion. In this method, the thermal limit of the transmission lines is identified in steady state and the stable economic operation of the power system is guaranteed. In [6], the locational marginal pricing has been used for determining the congestion contribution to the subnetworks of the power system.

Also, price area congestion management (PACM) is another traditional method of transmission congestion management based on the transmission network zoning [7]. Areas are formed in a way that the possibility of congestion inside the area is low or it is difficult to predict, and the probability of congestion between the areas is high. Also, in [8], a two-level optimization problem with the bidding strategy improvement approach is used in the congestion problem management. Congestion management is essentially a non-linear optimization program with multiple variables and constraints. Today, many researchers have used intelligent optimization algorithms such as genetic algorithms, particle swarm

* Corresponding author.
E-mail addresses: fariborz_z55@yahoo.com (F. Zaeim-Kohan), razmi.hadi@gmail.com (H. Razmi), hasan_doagou@yahoo.com (H. Doagou-Mojarrad).

https://doi.org/10.1016/j.asoc.2018.05.028
1568-4946/

Nomenclature

$(\alpha_p, \beta_p, \gamma_p)$ coefficients of the pth generator emission characteristics
(a_p, b_p, c_p) cost coefficient of the pth generator
Δd_m load reduction in the responsive bus m
$\mu_{f_\alpha(\boldsymbol{par}_\beta)}$ membership function for the αth objective function and the βth solution
ρ_0 and ρ the electricity prices, before and after implementation of DRPs, respectively
$\boldsymbol{bpar}_\beta$ the best solution achieved for the βth particle
$\boldsymbol{gpar}$ the best position found for all particles in the swarm
$\boldsymbol{n}_\mu$ the fuzzy normalized vector
$\boldsymbol{par}_\beta(t)$ location of the particle β at time t
$\boldsymbol{u}$ the vector of independent variables or control variables
$\boldsymbol{vel}_\beta(t)$ velocity of the particle β at time t
$\boldsymbol{x}$ the vector of state variables
θ_{qa} phase angle difference between buses q and a
B_{qa} susceptance of the admittance matrix entry qa
c_1 cognitive factor
c_2 social factor
cp_β cumulative probability of the βth solution
d_{0_m} and d_m the amount of load at mth responsive bus before and after the DR, respectively
E the load elasticity
$f_i(\boldsymbol{x}, \boldsymbol{u})$ the ith continuous objective function
$f_\alpha(\boldsymbol{par}_\beta)$ value of the αth objective function for the βth solution
$f_\alpha^{\min}$ and $f_\alpha^{\max}$ lower and upper limits of the αth objective function
$g_j(\boldsymbol{x}, \boldsymbol{u})$ the jth continuous equality constraint function
G_{qa} conductance of the admittance matrix entry qa
$h_k(\boldsymbol{x}, \boldsymbol{u})$ the kth continuous inequality constraint function
inc the incentive factor
inc_m the total incentive paid to the mth responsive bus for participating in DRPs
$inc_m^{\min}$ and $inc_m^{\max}$ minimum and maximum amount of the incentive at the responsive bus m
LR_m the load reduction requested by ISO, for mth responsive load
N_B number of buses
N_{BR} number of transmission lines
N_{DR} number of responsive demands
N_{eq} number of equality constraint functions
N_G number of generators
N_{ineq} number of inequality constraint functions
N_L number of load buses
N_{obj} number of objective functions
N_{par} number of optimization parameters
N_{rep} the number of solutions available in the repository
N_{swarm} population size
P_{D_q} active power demand of the bus q
P_{G_p} active power generation of the unit p
$P_{G_p}^{\min}$ and $P_{G_p}^{\max}$ lower and upper limits of active power generation of the unit p, respectively
par_{η_h} location of the parameter η in the particle h
$par_{\eta_h}^{\min}$ and $par_{\eta_h}^{\max}$ lower and upper limits of the parameter η in the particle h, respectively
pen the penalty factor
pen_m the total penalty for mth responsive load
Q_{D_q} reactive power demand of the bus q
Q_{G_p} reactive power generation of the unit p
$Q_{G_p}^{\min}$ and $Q_{G_p}^{\max}$ lower and upper limits of reactive power generation of the unit p, respectively
S_{l_n} apparent power flow of the transmission line n
$S_{l_n}^{\max}$ maximum thermal limit of the transmission line n
V_{G_p} voltage magnitude at the PV bus p
$V_{G_p}^{\min}$ and $V_{G_p}^{\max}$ lower and upper limits of voltage magnitude of the PV bus p, respectively
V_{L_r} voltage magnitude at the load bus r
$V_{L_r}^{\min}$ and $V_{L_r}^{\max}$ lower and upper limits of voltage magnitude of the load bus r, respectively
V_q voltage magnitude of the bus q
vel_{η_h} velocity of the parameter η in the particle h
w inertia factor
w_α weighting coefficient of the αth objective function
rand random real vector
DLC direct load control
DR demand response
DRPs demand response programs
DSM demand side management
EDRPs emergency demand response programs
EE energy efficiency
ISO independent system operator
MOPSO multi-objective particle swarm optimization
rand random real number
SR spinning reserve

optimization algorithms and other evolutionary algorithms to solve this problem [9–11].

In [10], an effective optimization technique namely Firefly algorithm has been proposed for the congestion problem management in an open access electricity market. In this paper, contingencies such as line outage and sudden load change are considered.

In [11], a new scheme has been suggested for estimating the transmission congestion pricing based on power flow tracing by employing PSO algorithm. Also, in [12], information gap decision theory has been employed to tackle congestion management problem using flexible capabilities of DG and demand response. In this paper, effective results are obtained based on congestion and voltage management in the presence of uncertainty.

The use of flexible AC transmission systems (FACTS) in congestion management has been mentioned in several articles [12,13]. With this equipment, the transmission line flows can be controlled without generation rescheduling or topological changes in the network, and in this way, system losses and generation costs are reduced and network stability increases.

Another idea in congestion management is using generation rescheduling units [14,15]. Doing so, some part of the capacity of congested lines is released and transferred to the non-congested lines.

As reported in [16], a new congestion management method was employed using generation rescheduling and load shedding with the voltage-dependent load modeling. In the paper, the objective functions of reducing load shedding and generation costs including minimizing load shed, increasing social welfare, and increasing the load served are discussed.

In [17], an efficient technique for congestion management is suggested which aimed at changing the generators output power plan considering pumped-storage hydropower plant unit in the power system. In this paper, an optimization model is proposed according to two generator and bus sensitivity factors. Optimal location of pumped-storage hydropower plant unit is detected using bus sensitivity factor amount and the number of generators contributing to congestion management, whose program has

been changed due to the generator sensitivity factor. The simulation results in the reduction of congestion costs and improvement of system security.

Demand side management (DSM) focuses on reduction in energy consumption and monetary incentives, mitigates the operations cost, saves fuel and minimizes the total congestion cost [18]. DSM can be categorized into the following based on the timing and the effect of the applied measures on the customer strategies:

- Energy efficiency (EE)
- Load shifting program
- Demand response (DR)
- Spinning reserve (SR)

DRP is one of the new, useful and efficient methods for transmission congestion management [19,20]. In advanced power markets, consumers are given the opportunity to respond to energy prices in the wholesale market and change their consumption proportional to the price fluctuations. In this way, subscribers will be able to help prevent lines congestion and participate in its management. In the case of subscribers participation in pricing their energy consumption, not only will the electricity demand curve be converted to a curve sensitive to electricity prices from a curve with a zero price elasticity, but also the use of market power by electricity producers will be reduced appropriately with the competition increase between power producers for more suitable pricing in the electricity market. DRPs prevent the adverse effects of the financial costs incurred and reduced social welfare. DRPs modeling is based on the price elasticity matrix, which is one of the most common and powerful methods in the field [21]. Demand response is highly recommended around the world due to its impressive benefits such as reduced cost and improved reliability. DRPs are divided into two main categories: incentive-based and time-based programs. In the same vein, In [22], a new method has been proposed based on DPRs optimal locations and time of implementation. In this case, by changing the price of electricity in different periods, customers are encouraged to modify their consumption patterns.

In [23], a new format has been proposed for congestion management using DRPs resources in the smart grid. In the proposed two-level structure, the system operator runs the electricity market regardless of transmission network limitations. Then, according to the transmission lines congestion, an interaction is considered between DRP and load shedding. Also, a complete overview of traditional and modern methods of congestion management is presented in [24].

Table 1 shows the comparison of our congestion management problem with other models investigated in the published papers.

This paper focuses on solving congestion management in which generation rescheduling, emergency demand response program (EDRP) and direct load control (DLC) during congested hour have been taken into consideration. In the present paper, a multi objective congestion management is formulated and in order to solve the problem, fuzzy multi objective particle swarm optimization (MOPSO) with Pareto solutions is proposed. The proposed multi objective model considers a variety of objective functions and technical issues including maximization of transmission lines loading, minimization of operating costs and emission reduction.

The main contributions of this paper are as follows:

(1) Providing a nonlinear mathematical model of incentive-based DRPs.
(2) Investigating the effects of DRPs on the fuel cost reduction, reduction of environmental pollution, losses as well as reduction of transmission lines congestion.

This paper consists of the following sections: in the second section, the multi-objective congestion management problem is expressed with its corresponding objective functions and different constraints. In the third section, multi-objective particle swarm optimization algorithm and its implementation will be explained. In the fourth section, using the proposed method, the problem of transmission congestion management is resolved in different scenarios and states, and the numerical results are presented for IEEE 30-bus and IEEE 118-bus test systems. Finally, section five concludes the paper.

2. Problem of multi-objective transmission congestion management

The problem of transmission congestion management can be expressed as multi-objective constrained nonlinear optimization problem as follows:

$$\begin{aligned} &\text{minimize} && f_i(\boldsymbol{x},\boldsymbol{u}); && i=1,\ldots,N_{obj} \\ &\text{subject to} && g_j(\boldsymbol{x},\boldsymbol{u})=0; && j=1,\ldots,N_{eq} \\ & && h_k(\boldsymbol{x},\boldsymbol{u})\le 0; && k=1,\ldots,N_{ineq} \end{aligned} \tag{1}$$

Different sections of this problem are defined in the following subsections.

2.1. Control variables

Transmission congestion management is done through changes in the value of these variables. Assuming that the index of slack bus

Table 1
Comparison of the proposed congestion management problem with other published paper.

	Objective function	Single or multi-objective	Solution method	Demand-side management	FACTS device
[9]	Congestion cost	Single	AANN and the modified PSO algorithm	DRP	Phase shifter transformers
[11]	Congestion cost	Single	PSO algorithm	–	–
[12]	Fuel and emission cost	Single	Bacterial foraging and Nelder Mead algorithm	–	TCSC
[13]	Total market/re-dispatch cost	Single	CPLEX under GAMS software	DRP	TCSC
[15]	Congestion cost	Single	Ant lion optimizer algorithm	–	–
[16]	Generation cost minimization/ amount of load shedding minimization	Multi-objective	Strength Pareto evolutionary algorithm 2+	Load shedding	–
Our paper	Increased transmission lines loading/reduction of operating costs of the power system/emissions reduction	Multi-objective	MOPSO	DRP	–

is 1, the control variables vector of the congestion management problem used in this paper are:

$$\boldsymbol{u}^T = [P_{G_2}, \ldots, P_{G_{N_G}}, \Delta d_1, \ldots, \Delta d_{N_{DR}}] \quad (2)$$

2.2. State variables

Presence of congestion in the power system is detected using the measured values of these variables. The set of these dependent variables which are called as the state variables vector, are:

$$\boldsymbol{x}^T = [P_{G_1}, V_{L_1}, \ldots, V_{L_{N_L}}, Q_{G_1}, \ldots, Q_{G_{N_G}}, S_{l_1}, \ldots, S_{l_{N_{BR}}}] \quad (3)$$

2.3. Objective functions

2.3.1. Transmission lines loading maximization

Aiming at increasing the loadability of the most congested transmission line, this function is defined as follows:

$$\text{minimize} \quad \max_n\{S_{l_n}\}; \quad n = 1, \ldots, N_{BR} \quad (4)$$

2.3.2. Generation cost minimization

Reduction of electricity generation costs, which are mainly related to the costs of fuel in power plants, is defined with the following function:

$$\text{minimize} \quad \sum_{p=1}^{N_G} a_p + b_p P_{G_p} + c_p P_{G_p}^2 \quad (5)$$

where, a_p, b_p and c_p are the cost coefficients of the pth generating unit.

2.3.3. Emissions minimization

Reducing the amount of emissions produced by power plants is another purpose that is defined by the following function:

$$\text{minimize} \quad \sum_{p=1}^{N_G} \alpha_p + \beta_p P_{G_p} + \gamma_p P_{G_p}^2 \quad (6)$$

where, α_p, β_p and γ_p are the pollution coefficients of the pth generating unit.

2.3.4. DR cost minimization

Demand response is generally defined as the participation of small consumers in the electricity market, facing with market spot prices and responding them. Two factors can lead to the acceptance of consumers' response: first, electricity price change is at the retail level, which reflects the changing nature of the real price of electricity; and second, the implementation of the incentive programs in order to satisfy the customers to reduce their consumption at critical times. This incentive can be reflected as a payment to the consumer for reducing the demand.

Demand response methods can be divided into two general categories as below [25]:

- Incentive-based DRPs
- Time-based DRPs

Fig. 1 shows the classification of demand response types. This paper is mainly focused on the common incentive based on emergency demand response programs (EDRPs), and direct load control (DLC).

For successful implementation of DRPs, a set of load buses must be selected based on their impacts on the transmission network loading.

Incentive-based:

- Emergency demand response program (EDRP)
- Direct Load Control (DLC)
- Interruptible/Curtailable Service (I/C)
- Ancillary Services Market (A/S)
- Capacity Market (CAP)
- Demand Bidding (DB)

Time-based:

- Time of Use (TOU)
- Real Time Pricing (RTP)
- Critical Peak Pricing (CPP)

Fig. 1. Classification of DRPs.

Hence, an elastic demand model is proposed based on incentive and penalty along with customer benefit function to estimate the demand response capacity. The change of mth response load, after the implementation of DRPs is expressed by the following equation:

$$\Delta d_m = d_{0_m} - d_m \quad (7)$$

where, d_{0_m} and d_m are the amount of load at mth response bus before and after the demand response, respectively.

If an amount of inc is paid to the customer for each unit of load reduction, the total incentive paid to the mth responsive bus for participating in DRPs is calculated by the following equation:

$$inc_m = inc \times [d_{0_m} - d_m] \quad (8)$$

If the customers participating in DRPS do not respond to the minimum reduced load required in the contract, they will be required to pay a penalty. If the load reduction requested by ISO, for mth responsive load shown by LR_m, the total penalty for mth responsive load can be calculated as follows:

$$pen_m = pen \times [LR_m - \Delta d_m] \quad (9)$$

Values of *inc* and *pen* are determined by the market operator. In this paper, *pen* factor is equal to zero, and *inc* coefficient is considered to be 0.1–10 times of the electricity price before implementation of DRPs.

To express the customer's revenue in terms of load, various functions such as linear, power, exponential, and logarithmic functions are suggested in various articles [21]. In this paper, linear responsive load model is used which can be expressed as follows:

$$d_m = d_{0_m} \times \left[1 + E \times \frac{\rho - \rho_0 + inc - pen}{\rho_0}\right] \quad (10)$$

where, E is the load elasticity, and ρ_0 and ρ are the electricity prices, before and after implementation of DRPs, respectively.

Therefore, the generation cost in addition to the amount of paid incentive to the set of responsive loads, is another goal finally calculated by the following equation:

$$\text{minimize} \quad \sum_{p=1}^{N_G} a_p + b_p P_{G_p} + c_p P_{G_p}^2 + \sum_{m=1}^{N_{DR}} inc_m \quad (11)$$

2.4. Equality constraints

The set of power flow equations, defined for the balance of active and reactive powers in the network as follows, form the equality

constraints of the optimization problem:

$$P_{G_q} - (P_{D_q} - d_q) - V_q \sum_{a=1}^{N_B} V_a (G_{qa} \cos\theta_{qa} + B_{qa} \sin\theta_{qa}); \quad q = 1, \ldots, N_B \tag{12}$$

$$Q_{G_q} - Q_{D_q} - V_q \sum_{a=1}^{N_B} V_a (G_{qa} \sin\theta_{qa} - B_{qa} \cos\theta_{qa}); \quad q = 1, \ldots, N_B \tag{13}$$

2.5. Inequality constraints

Authorized limits of control and state variables are determined by inequality constraints. In the following subsections, inequality constraints related to the various elements of the power system are presented.

2.5.1. Generator constraints

Active and reactive powers and voltages of each generator are limited between a lower and upper limit as follows:

$$V_{G_p}^{\min} \le V_{G_p} \le V_{G_p}^{\max}; \quad p = 1, \ldots, N_G \tag{14}$$

$$P_{G_p}^{\min} \le P_{G_p} \le P_{G_p}^{\max}; \quad p = 1, \ldots, N_G \tag{15}$$

$$Q_{G_p}^{\min} \le Q_{G_p} \le Q_{G_p}^{\max}; \quad p = 1, \ldots, N_G \tag{16}$$

2.5.2. Constraints of the incentive paid to the responsive loads

The incentive paid to each responsive load is restricted between a lower and upper limit as follows:

$$inc_m^{\min} \le inc_m \le inc_m^{\max}; \quad m = 1, \ldots, N_{DR} \tag{17}$$

2.5.3. Security constraints

The constraints related to the voltage of each power system load along with the constraints related to the thermal limit of transmission lines, are read in the name of security constraints of the power system and are defined as follows:

$$V_{L_r}^{\min} \le V_{L_r} \le V_{L_r}^{\max}; \quad r = 1, \ldots, N_L \tag{18}$$

$$S_{l_n} \le S_{l_n}^{\max}; \quad n = 1, \ldots, N_{BR} \tag{19}$$

It should be noted that in the problem of transmission congestion management, the control variables of the power system are defined before the study of power flow within the allowable limits and that each of the power system state variables may go out of the allowed range after the study of power flow. If at least one state variable goes out of its allowed range, the amount of each of the objective functions will increase by adding a large penalty, in order to remove that response from the set of acceptable responses.

$$f_i(\boldsymbol{x}, \boldsymbol{u}) = f_i(\boldsymbol{x}, \boldsymbol{u}) + penalty; \quad i = 1, \ldots, N_{obj} \tag{20}$$

3. Multi-objective congestion management using MOPSO algorithm

In the multi-objective optimization problems with numerous objectives, sorting the set of responses is very complicated. The primary methods proposed so far have converted a multi-objective problem into a single-objective problem. However, these methods can have many limitations including large amounts of computation, the need for prior knowledge of the problem, and determining the weighted values of the objective function. In the multi-objective problems, there is not only one solution, but a set of solutions is obtained called the Pareto optimal set [26,27]. This name is chosen based on the name of Wilfred Pareto, a famous economist, who presented the Pareto optimality theory.

The main advantage of multi-objective evolutionary optimization algorithms is their ability to model the non-dominated solutions simultaneously. Therefore, they have the ability to estimate the set of optimal solutions (Pareto front) rather than a single optimal solution in each implementation of algorithm. Over the past years, researchers have presented several methods for solving the multi-objective optimization problems with the help of evolutionary algorithms. Therefore, multi-objective particle swarm optimization algorithm, as the method used in this paper, is explained to solve the problem of multi-objective congestion management.

3.1. Implementation of MOPSO algorithm

Multi-objective optimization with conflicting objective functions results in a set of solutions rather than an optimized solution. The optimality of a large number of solutions is that, taking into account all objective functions simultaneously, no solution can optimize all objective functions.

In order to implement the multi-objective particle swarm optimization algorithm in the congestion management of power systems, the following steps are run:

Step 1. Information call

At this step, the following information is called: information of data transmission lines and generation units such as resistance and reactance of lines, thermal limit of transmission lines, lines length, cost and emission coefficients of generators, the generators constraints, information on responsive loads, as well as the load demand.

Step 2. Generation of the initial population for the location and velocity of the particles

To start the algorithm, like any other evolutionary algorithm, an initial population must be generated randomly to meet all the restrictions listed as follows:

Random generation of particles location:

$$POP = \left[\boldsymbol{u}_1^T, \ldots, \boldsymbol{u}_{N_{swarm}}^T\right]^T \tag{21}$$

$$\begin{aligned} \boldsymbol{par}_h^T = \boldsymbol{u}_h^T &= [P_{G_{2_h}}, \ldots, P_{G_{N_{Gh}}}, \Delta d_{1_h}, \ldots, \Delta d_{N_{DR_h}}] \\ &= [par_{1_h}, \ldots, par_{N_{par_h}}]; \quad h = 1, \ldots, N_{swarm} \end{aligned} \tag{22}$$

$$par_{\eta_h} = par_{\eta_h}^{\min} + \text{rand} \times (par_{\eta_h}^{\max} - par_{\eta_h}^{\min}); \quad \eta = 1, \ldots, N_{par} \tag{23}$$

Random generation of particles velocity:

$$VEL = \left[\boldsymbol{vel}_1^T, \ldots, \boldsymbol{vel}_{N_{swarm}}^T\right]^T \tag{24}$$

$$\boldsymbol{vel}_h^T = [vel_{1_h}, \ldots, vel_{N_{par_h}}]; \quad h = 1, \ldots, N_{swarm} \tag{25}$$

$$vel_{\eta_h} = 0.1 \times [par_{\eta_h}^{\min} + \text{rand} \times (par_{\eta_h}^{\max} - par_{\eta_h}^{\min})]; \quad \eta = 1, \ldots, N_{par} \tag{26}$$

Step 3. Meeting the constraints

At this step, since the particles are randomly generated, the equality and inequality constraints must be controlled.

Step 4. Calculation of objective functions

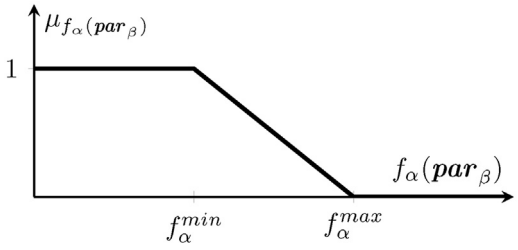

Fig. 2. Membership function of the objective function.

For each population, the objective functions (4), (6) and (11) are calculated. In the case of both of the following conditions, $\boldsymbol{par}_1$ solution will dominate $\boldsymbol{par}_2$ solution.

1. For each of the objective functions, the value of function for $\boldsymbol{par}_1$ solution is less than or equal to the value of $\boldsymbol{par}_2$. Mathematically:

$$\forall z \in \{1, \ldots, N_{obj}\}, \quad f_z(\boldsymbol{par}_1) \le f_z(\boldsymbol{par}_2) \tag{27}$$

2. At least for one objective function, the value of function for $\boldsymbol{par}_1$ solution is less than the value of function for $\boldsymbol{par}_2$. Mathematically:

$$\exists v \in \{1, \ldots, N_{obj}\}, \quad f_v(\boldsymbol{par}_1) < f_v(\boldsymbol{par}_2) \tag{28}$$

If $\boldsymbol{par}_1$ dominates $\boldsymbol{par}_2$, $\boldsymbol{par}_1$ will be saved as a dominant solution in the repository. The solution available in the repository will form the Pareto curve. In order to place the solution in the repository, the following conditions must be observed:

- Repository is not full.
- The desired solution is not dominated by any of the solutions available in the repository.

Since in this method, there is a set of solutions to control the size of the repository and at the same time to choose better responses among the non-dominated solutions which have a good compromise with all objective functions, fuzzy clustering method is used.

Step 5. Determining the fuzzy membership functions

Membership function $\mu_{f_\alpha(\boldsymbol{par}_\beta)}$ for the αth objective function and βth solution in shown in Fig. 2.

Membership functions of each of the objective functions are achieved according to its minimum and maximum values. Minimum and maximum values of objective functions are determined by implementing one of the single-objective optimization methods.

The numerical value obtained from the membership function shows the operator satisfaction, in a way that if $\mu_{f_\alpha(\boldsymbol{par}_\beta)} = 1$ is obtained for the function of $f_\alpha(\boldsymbol{par}_\beta)$, the operator has the highest satisfaction with the βth solution, and if the value is zero, it shows the operator's minimum satisfaction. The following equation shows the calculation of $\mu_{f_\alpha(\boldsymbol{par}_\beta)}$ for the αth objective function.

$$\mu_{f_\alpha(\boldsymbol{par}_\beta)} = \begin{cases} 0 & f_\alpha(\boldsymbol{par}_\beta) > f_\alpha^{\max}, \\ \dfrac{f_\alpha^{\max} - f_\alpha(\boldsymbol{par}_\beta)}{f_\alpha^{\max} - f_\alpha^{\min}} & f_\alpha^{\min} \le f_\alpha(\boldsymbol{par}_\beta) \le f_\alpha^{\max}, \\ 1 & f_\alpha(\boldsymbol{par}_\beta) < f_\alpha^{\min}. \end{cases} \tag{29}$$

After obtaining the membership functions for each objective, for the βth solution, the fuzzy normalized value of $n_\mu(\beta)$ is calculated as follows:

$$n_\mu(\beta) = \frac{\sum_{\alpha=1}^{N_{obj}} w_\alpha \times \mu_{f_\alpha(\boldsymbol{par}_\beta)}}{\sum_{\beta=1}^{N_{rep}} \sum_{\alpha=1}^{N_{obj}} w_\alpha \times \mu_{f_\alpha(\boldsymbol{par}_\beta)}} \quad \beta = 1, \ldots, N_{rep} \tag{30}$$

In Eq. (30), N_{rep} and w_α are the number of solutions available in the repository, and weighting coefficient of the αth objective function, respectively. Then, the solutions are sorted in ascending order based on the value obtained for the normalized vector, and the responses in the bottom of the list are discarded based on the size of the repository.

Step 6. Updating the velocity and location of particles

New velocity and location of particles are determined by the following formula.

$$\boldsymbol{vel}_\beta(t+1) = w \times \boldsymbol{vel}_\beta(t) + c_1 \times \mathbf{rand} \times (\boldsymbol{bpar}_\beta - \boldsymbol{par}_\beta(t)) + c_2 \times \mathbf{rand} \times (\boldsymbol{gpar} - \boldsymbol{par}_\beta(t)) \tag{31}$$

$$\boldsymbol{par}_\beta(t+1) = \boldsymbol{vel}_\beta(t+1) + \boldsymbol{par}_\beta(t) \quad \beta = 1, \ldots, N_{swarm} \tag{32}$$

Step 7. Meeting the constraints

It is noteworthy that since at each step in which a new population is made, equality and inequality constraints must be checked, the stages mentioned in the fourth step are also performed at this step.

Step 8. Updating $\boldsymbol{bpar}_\beta$ and $\boldsymbol{gpar}$

For the populations obtained from the seventh step, the values of the objective function are calculated; then, $\boldsymbol{bpar}_\beta$ will be updated using the following equation.

- If the solution of $\boldsymbol{par}_\beta(t+1)$ dominates the solution of $\boldsymbol{bpar}_\beta$, it will be replaced by $\boldsymbol{bpar}_\beta$.
- If the solution of $\boldsymbol{bpar}_\beta$ dominates the solution of $\boldsymbol{par}_\beta(t+1)$, $\boldsymbol{bpar}_\beta$ will remain unchanged.
- If the solutions of $\boldsymbol{par}_\beta(t+1)$ and $\boldsymbol{bpar}_\beta$ do not dominate each other, one of the solutions will be considered randomly as $\boldsymbol{bpar}_\beta$.

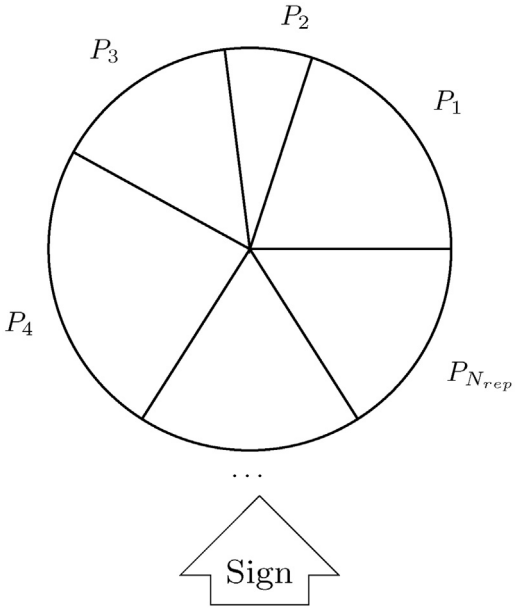

Fig. 3. Simplified schematic of roulette wheel.

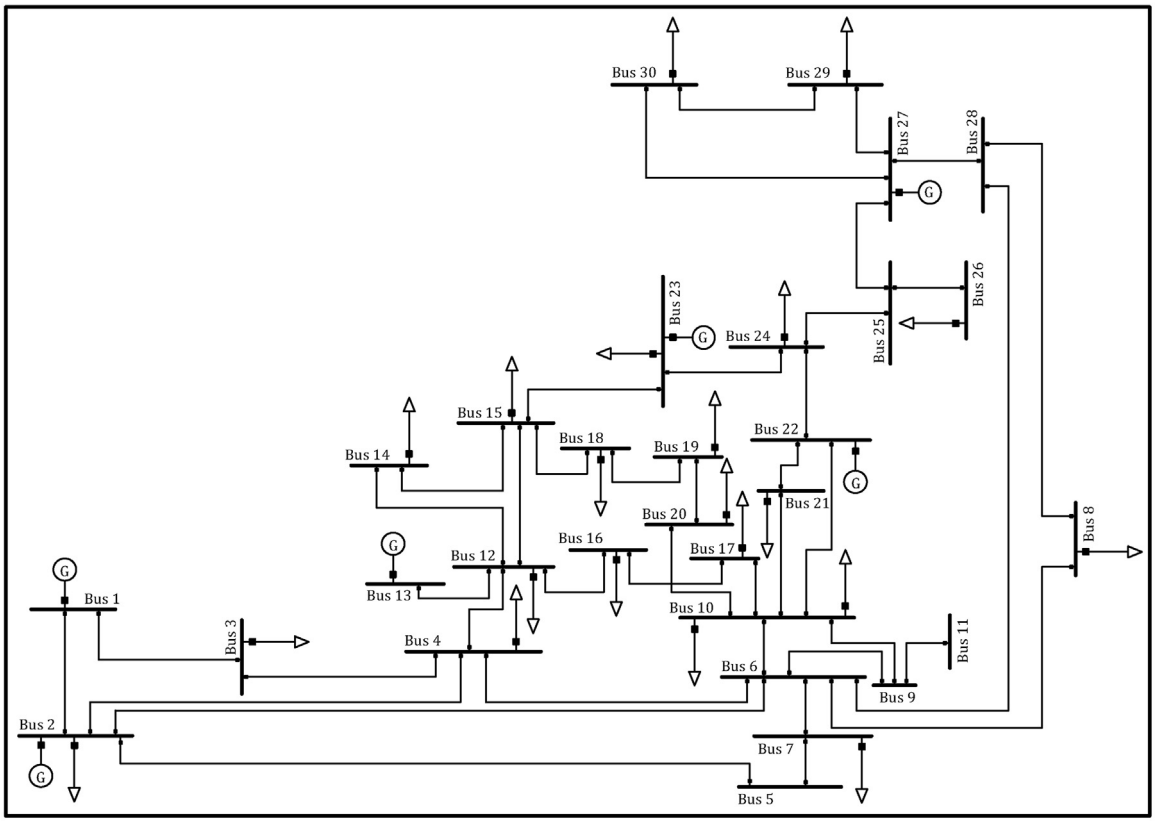

Fig. 4. Single-line diagram of a standard IEEE 30-bus test system.

Value of ***gpar*** will be calculated and updated as follows:

In this method, ***gpar*** is selected from the solutions available in the repository. In this equation, the following stages will be implemented by selecting ***gpar***.

1. Fuzzy normalized vector for the solutions available in the repository will be formed as the following:

$$\boldsymbol{n}_{\mu}^{T} = [n_{\mu}(1), \ldots, n_{\mu}(N_{rep})] \tag{33}$$

2. For the vectors derived from the previous stage, cumulative probabilities are calculated as follows:

$$\begin{aligned} cp_1 &= n_{\mu}(1) \\ cp_2 &= cp_1 + n_{\mu}(2) \\ &\vdots \\ cp_{N_{rep}} &= cp_{N_{rep}-1} + n_{\mu}(N_{rep}) \end{aligned} \tag{34}$$

3. At this stage, ***gpar*** is selected by the roulette wheel. Roulette wheel is a method for selecting a state from among a number of certain states based on the probability of that state. Roulette wheel is a wheel that is divided into several sectors. Each sector corresponds to an event from a collection of events, and its circumference is proportional to the probability of that event. Fig. 3 shows a simplified schematic of the roulette wheel.

   If the wheel moves, regardless of speed, acceleration and the beginning point of the wheel movement, the probability that the mark is placed in the range of each of the sectors of the wheel, will be equal to the probability corresponding to the sector. Random number of rand plays the role of the mark in the above figure. According to the previous equation, the amount of cumulative probability for the first solution is equal to the fuzzy normalized value of that solution, and it is equal to 1 for the last solution. Generating the random number of rand, which has a value between 0 and 1, and comparing it with cumulative probability values, the solution corresponding to the cumulative probability value is considered as ***gpar***.

Step 9. Termination condition

There are several methods to finish the program. In this paper, the conditions for achieving the maximum iteration are used.

4. Simulation results

In this section, to evaluate the proposed method, two case studies (IEEE 30-bus and IEEE 118-bus test systems) of congestion management problem will be discussed.

4.1. IEEE 30-bus test system

The single-line diagram of the network is shown in Fig. 4. This network has 20 loads, 6 generators, and 41 transmission lines. Network generators are located at buses 1, 2, 13, 22, 23, and 27.

The amount of the active and reactive power demands, the maximum and minimum power of generators and the information of transmission lines within its allowable limits, are given in Tables 2–4 [12].

In the transmission lines congestion management, load buses Nos. 7, 8, 12, 17, 19, 21, and 30 have been selected to participate in DRPs, based on generation shift factor (GSF) [13]. It is assumed that each of the responsive demand buses can reduce its load up to 10%. Also, the market price before and after the implementation of demand response is assumed to be 50 $/MW [19]. Elasticity coefficient of E for all responsive demands is considered to be equal to −0.1 [13].

Table 2
Bus data for the IEEE 30-bus test system.

Bus no.	Bus type	Power demand		Power generation	
		Active [MW]	Reactive [Mvar]	Active [MW]	Reactive [Mvar]
1	Slack	0	0	1.05	0.95
2	PV	21.7	12.7	1.05	0.95
3	PQ	2.4	1.2	1.05	0.9
4	PQ	7.6	1.6	1.05	0.9
5	PQ	0	0	1.05	0.9
6	PQ	0	0	1.05	0.9
7	PQ	22.8	10.9	1.05	0.9
8	PQ	30	30	1.05	0.9
9	PQ	0	0	1.05	0.9
10	PQ	5.8	2	1.05	0.9
11	PQ	0	0	1.05	0.9
12	PQ	11.2	7.5	1.05	0.9
13	PV	0	0	1.05	0.95
14	PQ	6.2	1.6	1.05	0.9
15	PQ	8.2	2.5	1.05	0.9
16	PQ	3.5	1.8	1.05	0.9
17	PQ	9	5.8	1.05	0.9
18	PQ	3.2	0.9	1.05	0.9
19	PQ	9.5	3.4	1.05	0.9
20	PQ	2.2	0.7	1.05	0.9
21	PQ	17.5	11.2	1.05	0.9
22	PV	0	0	1.05	0.95
23	PV	3.2	1.6	1.05	0.95
24	PQ	8.7	6.7	1.05	0.9
25	PQ	0	0	1.05	0.9
26	PQ	3.5	2.3	1.05	0.9
27	PV	0	0	1.05	0.95
28	PQ	0	0	1.05	0.9
29	PQ	2.4	0.9	1.05	0.9
30	PQ	10.6	1.9	1.05	0.9

Table 3
Generation data for the IEEE 30-bus test system.

Code	Bus no.	Generation limits			
		Max [MW]	Min [MW]	Max [Mvar]	Min [Mvar]
G1	1	80	0	150	−20
G2	2	80	0	60	−20
G3	22	50	0	62.5	−15
G4	27	55	0	48.7	−15
G5	23	30	0	40	−10
G6	13	40	0	44.7	−15

Information of cost function coefficients and emission function coefficients in Eqs. (9) and (10), for generators in the test system, are given in Table 5.

Results of the transmission line flows, regardless of the thermal limit of transmission lines, are shown in Table 6.

As the results of this table show, the apparent power flow of the transmission lines Nos. 10 and 16, are equal to 34.83 and 38.7 MVA, respectively; and thus, given the numbers 30, 32, and 35 MVA, for the maximum thermal limit of the transmission lines, at least one of these lines is congested. In this paper, to relieve congestion in transmission lines, the generation rescheduling control strategy and DRPs were used in the following five scenarios.

- The problem of congestion management by taking into account the generation rescheduling control strategy and regardless of DRPs. In this scenario, the maximum thermal limit of the transmission lines is considered to be 35 MVA.
- The problem of congestion management by taking into account the generation rescheduling control strategy and DRPs. In this scenario, the maximum thermal limit of the transmission lines is also considered to be 35 MVA.

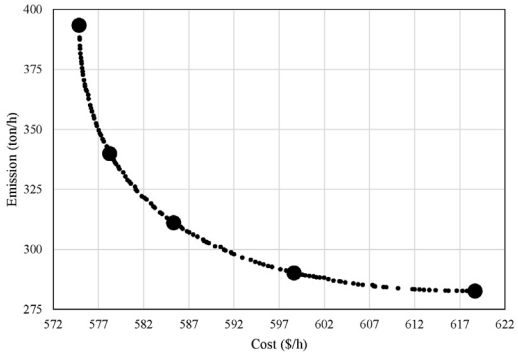

Fig. 5. Pareto curve of scenario 1.

- The problem of congestion management with control strategies similar to scenario 1, and with the maximum thermal limit of 32 MVA.
- The problem of congestion management with control strategies similar to scenario 2, and with the maximum thermal limit of 32 MVA.
- The problem of congestion management with control strategies similar to scenario 2, and with the maximum thermal limit of 30 MVA.

The multi-objective particle swarm optimization algorithm was implemented for objective functions of minimizing the total operating costs and reduction of emissions and Pareto curve for the above scenarios are respectively shown in Figs. 5–9.

It should be noted that in each of these scenarios, 120 Pareto solutions are obtained and multi-objective particle swarm optimization algorithm has been implemented with the parameters listed in Table 7.

Table 4
Line data for the IEEE 30-bus test system.

Line no.	Bus no.		Impedances [p.u.]			Line no.	Bus no.		Impedances [p.u.]		
	From	To	*R*	*X*	*B*		From	To	*R*	*X*	*B*
1	1	2	0.02	0.06	0.03	22	15	18	0.11	0.22	0
2	1	3	0.05	0.19	0.02	23	18	19	0.06	0.13	0
3	2	4	0.06	0.17	0.02	24	19	20	0.03	0.07	0
4	3	4	0.01	0.04	0	25	10	20	0.09	0.21	0
5	2	5	0.05	0.2	0.02	26	10	17	0.03	0.08	0
6	2	6	0.06	0.18	0.02	27	10	21	0.03	0.07	0
7	4	6	0.01	0.04	0	28	10	22	0.07	0.15	0
8	5	7	0.05	0.12	0.01	29	21	22	0.01	0.02	0
9	6	7	0.03	0.08	0.01	30	15	23	0.1	0.2	0
10	6	8	0.01	0.04	0	31	22	24	0.12	0.18	0
11	6	9	0	0.21	0	32	23	24	0.13	0.27	0
12	6	10	0	0.56	0	33	24	25	0.19	0.33	0
13	9	11	0	0.21	0	34	25	26	0.25	0.38	0
14	9	10	0	0.11	0	35	25	27	0.11	0.21	0
15	4	12	0	0.26	0	36	28	27	0	0.4	0
16	12	13	0	0.14	0	37	27	29	0.22	0.42	0
17	12	14	0.12	0.26	0	38	27	30	0.32	0.6	0
18	12	15	0.07	0.13	0	39	29	30	0.24	0.45	0
19	12	16	0.09	0.2	0	40	8	28	0.06	0.2	0.02
20	14	15	0.22	0.2	0	41	6	28	0.02	0.06	0.01
21	16	17	0.08	0.19	0	–	–	–	–	–	–

Table 5
Cost and emission coefficients for the IEEE 30-bus test system.

Generator	*a* [$/h]	*b* [$/MWh]	*c* [$/MWh^2]	α [ton/h]	β [ton/MWh]	γ [ton/MWh^2]
G1	0	2	0.02	0.04091	−0.05554	0.0649
G2	0	1.75	0.0175	0.02543	−0.06047	0.05638
G3	0	1	0.0625	0.04258	−0.05094	0.04586
G4	0	3.25	0.00834	0.05326	−0.0355	0.0338
G5	0	3	0.025	0.04258	−0.05094	0.04586
G6	0	3	0.025	0.06131	−0.05555	0.05151

Table 6
The results of the power flow of the transmission lines in the basic case, without considering the maximum thermal constraint.

Line no.	Power flow			Line no.	Power flow		
	[MW]	[Mvar]	[MVA]		[MW]	[Mvar]	[MVA]
1	10.89	5.09	12.02	22	9.16	0.76	9.2
2	15.08	5.57	16.08	23	5.87	0.38	5.88
3	16.07	6.66	17.39	24	3.66	3.8	5.28
4	12.56	4.37	13.3	25	5.92	4.62	7.51
5	13.79	6.03	15.05	26	3.37	8.01	8.69
6	20.28	8.5	21.99	27	2.28	11.77	11.99
7	22.5	11.38	25.22	28	3.82	8.62	9.42
8	13.68	6.88	15.31	29	19.87	23.16	30.51
9	9.27	4.02	10.11	30	8.91	5.47	10.46
10	24.82	24.43	34.83	31	2.18	7.8	8.1
11	5.79	3.46	6.74	32	7.09	0.88	7.14
12	3.31	2	3.87	33	3.89	1.77	4.27
13	0	0	0	34	3.55	2.37	4.27
14	5.79	3.51	6.77	35	7.5	0.78	7.54
15	1.67	2.04	2.64	36	6.11	6.4	8.85
16	37	11.35	38.7	37	6.17	1.68	6.4
17	5.39	0.88	5.46	38	7.12	1.67	7.32
18	9.48	1.19	9.55	39	3.68	0.61	3.73
19	9.26	0.28	9.27	40	5.34	6.08	8.1
20	0.85	0.8	1.17	41	0.77	2.7	2.81
21	5.68	2.15	6.08	–	–	–	–

In these figures, five points are marked and determined based on weighting coefficients presented in Eq. (30) in accordance with Table 8.

Observing Figs. 5–9, the following results are achieved:

- Result of the case 1 in scenario 2 compared to case 1 in scenario 1 showed that in addition to having lower costs, it has lower emissions. Comparing case 1 in scenarios 3 and 4, similar results are observed. This means that, taking into account DRPs, they fulfill the objective of achieving the lowest cost better.
- Result of the case 5 in scenario 2 compared to case 5 in scenario 1 illustrated that in addition to having higher costs, it has lower emissions. Comparing the same case in scenarios 3 and 4, similar results are observed. Therefore, taking into account DRPs, they can fulfill the objective of reducing environmental pollution better.

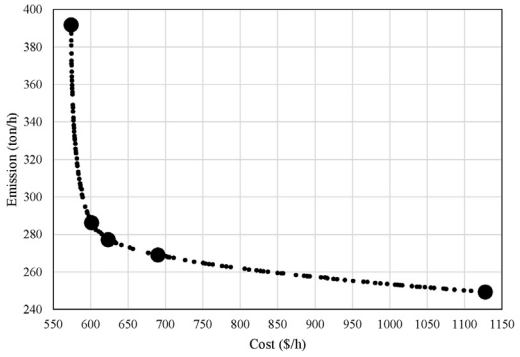

Fig. 6. Pareto curve of scenario 2.

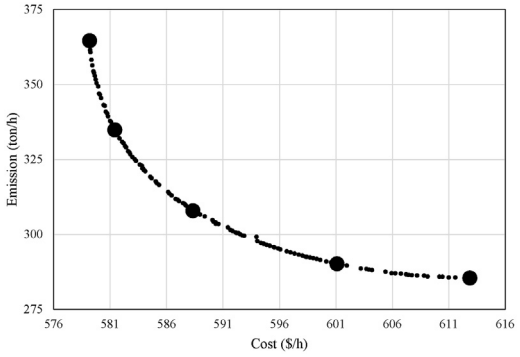

Fig. 7. Pareto curve of scenario 3.

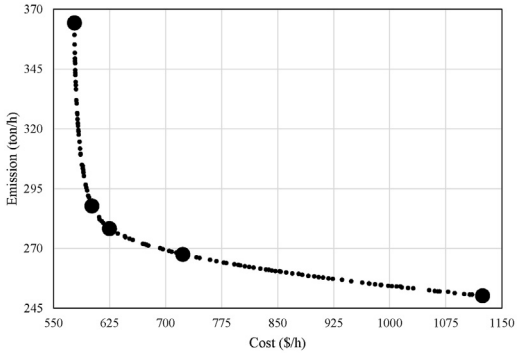

Fig. 8. Pareto curve of scenario 4.

Table 7
Parameters of multi-objective particle swarm optimization algorithm.

Parameter	Value
Inertia factor (w)	1
Cognitive factor (c_1)	2
Social factor (c_2)	2
Population size (N_{swarm})	200
Maximum number of iteration	120

Numerical results of generation scheduling, the reduction of responsive loads and the numerical value of objective functions of cost and emission, in different cases and in each of these five scenarios, are respectively expressed in Tables 9–11.

Moreover, to show the effects of using DRPs on the objective functions of cost and emission, Pareto curves of scenarios 3 and 4 are compared in Fig. 10.

The most important results obtained from Tables 9–11 and Fig. 10 are as follows:

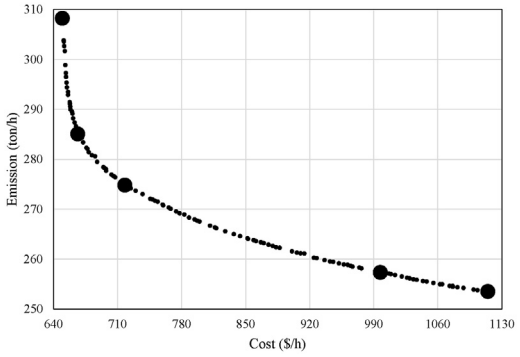

Fig. 9. Pareto curve of scenario 5.

Table 8
Weighting coefficients of objective functions of cost and emission.

	Case 1	Case 2	Case 3	Case 4	Case 5
Cost function coefficient (w_1)	1	0.75	0.5	0.25	0
Emission function coefficient (w_2)	0	0.25	0.5	0.75	1

Table 9
Numerical results of generation rescheduling in terms of MW.

		P_{G_1}	P_{G_2}	P_{G_3}	P_{G_4}	P_{G_5}	P_{G_6}
Scenario 1	Case 1	43.83	58.00	23.10	32.57	16.85	17.36
	Case 2	38.22	49.05	24.52	38.28	20.43	21.05
	Case 3	33.22	43.04	26.05	41.32	24.04	23.79
	Case 4	28.70	35.11	28.14	44.01	28.30	27.18
	Case 5	23.79	27.92	33.99	45.40	30.00	30.30
Scenario 2	Case 1	43.76	57.90	23.07	32.43	16.80	17.31
	Case 2	28.63	34.28	28.19	42.48	30.00	26.98
	Case 3	25.61	30.15	30.61	44.56	29.90	28.37
	Case 4	24.16	28.33	31.85	44.05	29.80	28.59
	Case 5	22.14	25.84	31.90	41.88	30.00	28.32
Scenario 3	Case 1	40.18	51.51	23.19	45.88	16.16	15.23
	Case 2	37.14	46.48	23.87	45.43	19.30	19.72
	Case 3	32.39	40.96	25.68	45.52	23.29	23.90
	Case 4	27.88	34.55	28.81	46.09	27.82	26.59
	Case 5	24.72	29.64	30.19	48.93	29.97	28.42
Scenario 4	Case 1	39.64	52.64	23.63	44.23	15.87	15.49
	Case 2	26.85	35.07	28.33	46.72	27.32	26.50
	Case 3	25.24	30.31	30.19	46.40	29.74	27.58
	Case 4	24.43	27.57	31.18	44.86	30.00	28.24
	Case 5	21.93	26.34	31.06	43.03	29.99	28.05
Scenario 5	Case 1	31.81	38.84	23.81	53.84	25.23	16.21
	Case 2	25.72	33.95	25.08	52.37	28.29	23.30
	Case 3	24.91	30.39	26.92	51.60	28.51	24.50
	Case 4	23.16	27.26	28.87	48.81	28.89	25.05
	Case 5	23.42	26.73	28.99	48.73	27.67	25.07

Table 10
Numerical results of load reduced in responsive loads in terms of MW.

		Bus 7	Bus 8	Bus 12	Bus 17	Bus 19	Bus 21	Bus 30
Scenario 2	Case 1	0.09	0.12	0.04	0.04	0.04	0.07	0.04
	Case 2	0.19	0.29	0.00	0.11	0.08	0.18	0.06
	Case 3	0.41	0.51	0.20	0.25	0.21	0.35	0.24
	Case 4	0.82	1.12	0.46	0.40	0.41	0.70	0.45
	Case 5	2.05	2.70	1.01	0.81	0.86	1.58	0.95
Scenario 4	Case 1	0.13	0.21	0.05	0.04	0.05	0.07	0.05
	Case 2	0.16	0.28	0.07	0.06	0.12	0.14	0.10
	Case 3	0.47	0.67	0.19	0.19	0.19	0.35	0.15
	Case 4	0.96	1.26	0.51	0.48	0.49	0.82	0.54
	Case 5	2.05	2.69	0.99	0.81	0.86	1.58	0.95
Scenario 5	Case 1	0.14	1.84	0.06	0.07	0.02	0.08	0.08
	Case 2	0.31	1.87	0.15	0.16	0.16	0.26	0.17
	Case 3	0.81	2.00	0.31	0.33	0.37	0.66	0.29
	Case 4	1.61	2.61	0.91	0.74	0.74	1.35	0.81
	Case 5	2.05	2.70	1.01	0.81	0.86	1.58	0.89

Table 11
Numerical results of objective functions of cost and emission.

		Case 1	Case 2	Case 3	Case 4	Case 5
Scenario 1	Generation cost [$/h]	574.87	578.27	585.32	598.66	618.68
	DR cost [$/h]	0.00	0.00	0.00	0.00	0.00
	Emission [ton/h]	393.38	339.86	311.04	290.15	282.59
Scenario 2	Generation cost [$/h]	573.18	596.81	600.82	596.01	574.74
	DR cost [$/h]	0.84	4.45	22.75	94.06	553.00
	Emission [ton/h]	391.79	286.29	277.12	268.98	249.25
Scenario 3	Generation cost [$/h]	579.18	581.42	588.33	601.09	612.86
	DR cost [$/h]	0.00	0.00	0.00	0.00	0.00
	Emission [ton/h]	364.53	334.79	307.80	290.15	285.44
Scenario 4	Generation cost [$/h]	576.26	597.17	601.35	593.98	574.62
	DR cost [$/h]	1.64	4.07	23.45	129.13	549.74
	Emission [ton/h]	364.27	287.75	278.27	267.47	250.18
Scenario 5	Generation cost [$/h]	583.38	590.13	588.08	575.59	569.85
	DR cost [$/h]	66.26	76.24	129.96	421.73	544.97
	Emission [ton/h]	308.22	285.09	274.80	257.31	253.51

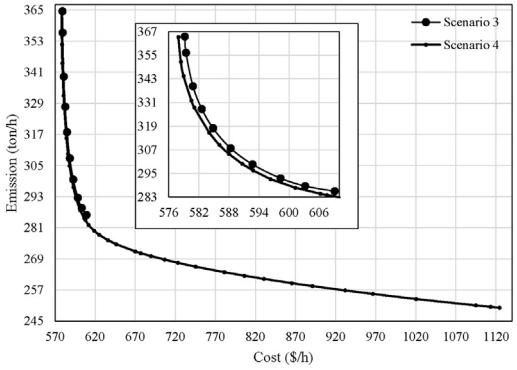

Fig. 10. Comparing the Pareto curves of scenarios 3 and 4.

- According to the numbers listed in Table 5, if the problem of cost is primarily important, cheaper power plants will be operated more, while considering the issue of reducing environmental pollution as the main objective, more expensive power plants will be used more.
- Comparing the results of the scenarios 1 and 2 shows that with DRPs, the total cost of operation are reduced. In fact, using DRPs, the share of generation of expensive generators decreases. This is clearly visible by comparing scenarios 3 and 4.
- Comparing the results of the scenarios 1 and 2 shows that using DRPs has also reduced the emissions. Obviously, the use of DRPs reduces the share of generation of power plants and as a result, it reduces their emissions. Similar results were also observed by comparing scenarios 3 and 4.

The MVA flow of three more congested lines Nos. 10, 16 and 29 for each of the five scenarios in different cases, is shown in Table 12.

It should be noted that by defining the number 30 MVA for the maximum thermal limit of the transmission lines, using the generation rescheduling and without using DRPs, solving the transmission congestion management problem is impossible. In Section 4.2, this issue has been discussed.

4.2. Discussion and comparison of the results

Since the issue of congestion management with the scenarios expressed has not been mentioned in any other paper, in order to assess and display the effects of DRPs on the problem of transmission lines congestion management, objective functions of increasing the loading of transmission lines and reducing the total cost of generation and implementation of DRPs are considered together. For this purpose, in Fig. 11, Pareto curves for objective functions (4) and (11) are compared in the cases with and without using DRPs.

Table 12
Numerical results of apparent power flow of more congested transmission lines in terms of MVA.

		Case 1	Case 2	Case 3	Case 4	Case 5
Scenario 1	Line 10	34.22	33.45	33.05	32.81	32.62
	Line 16	23.54	27.41	30.30	32.42	34.56
	Line 29	27.68	29.91	30.08	31.57	34.86
Scenario 2	Line 10	34.15	32.57	32.15	31.72	30.67
	Line 16	23.51	34.80	34.51	33.63	34.63
	Line 29	27.63	30.43	32.43	33.81	34.00
Scenario 3	Line 10	31.99	31.99	31.98	31.95	31.87
	Line 16	30.11	30.75	31.92	31.50	31.82
	Line 29	29.80	30.28	31.15	31.56	31.56
Scenario 4	Line 10	31.96	31.88	31.88	31.64	30.51
	Line 16	25.93	30.71	30.50	31.18	31.69
	Line 29	30.35	31.27	31.42	31.82	31.80
Scenario 5	Line 10	29.99	29.97	29.99	29.96	29.95
	Line 16	26.36	29.70	29.87	29.88	29.67
	Line 29	29.41	29.90	29.93	29.96	29.93

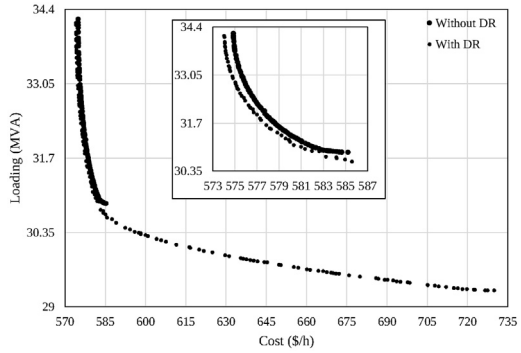

Fig. 11. Comparing the Pareto curves of objective functions of cost and loading in cases with and without DRPs.

Table 13
Numerical results of power transmission system losses in terms of MW.

	Case 1	Case 2	Case 3	Case 4	Case 5
Scenario 1	2.51	2.35	2.26	2.25	2.20
Scenario 2	2.50	2.28	2.21	2.13	1.94
Scenario 3	2.95	2.73	2.54	2.54	2.67
Scenario 4	2.88	2.50	2.52	2.39	2.22
Scenario 5	2.94	2.75	2.67	2.46	2.38

As can be seen in this figure, in the case without using DRPs, maximum thermal limit of the transmission lines cannot be considered less than 30.87 MVA. This is while in the case of using DRPs, maximum thermal limit of the transmission lines could be considered more than 29.3 MVA. This means that utilizing DRPs reduces the congestion of power system transmission lines, and allows the use of transmission lines with less loading capacity.

Also, the changes of power transmission system losses have been compared in five scenarios in Table 13.

As expected, the highest losses were in scenarios 1 and 3, in which DRPs were not used. In other scenarios, transmission system losses were reduced by decreasing the amount of the system load using DRPs.

Finally, in order to assess the suggested method, the obtained results are compared with those of the methods proposed in the

Table 14
The results of the comparison between the proposed method with those of the methods proposed in the literature [12] (the IEEE 30-bus system).

		Generation [MW]						Costs [$/h]		
		P_{G_1}	P_{G_2}	P_{G_3}	P_{G_4}	P_{G_5}	P_{G_6}	Fuel	Other	Total
Without emission	BF-NM [12]	42.47	63.63	41.61	11.84	12.59	20.47	606.31	42.6	648.86
	MOPSO (Scenario 3)	40.18	51.51	23.19	45.88	16.16	15.23	579.18	0	579.18
	MOPSO (Scenario 4)	39.64	52.64	23.63	44.23	15.87	15.49	576.26	1.64	577.90
With emission	GA [12]	44.33	53.27	37.43	19.21	16.64	22.82	1021.8	48.8	1070.6
	DE [12]	59.55	54.04	34.37	14.39	12.84	17.66	1028.7	44.9	1073.6
	PSO [12]	44.71	52.92	37.83	18.96	18.27	20.33	1017.9	47.8	1065.7
	BFA [12]	45.55	64.46	29.45	10.83	14.32	27.66	1022.0	53.4	1075.4
	BF-NM [12]	45.99	56.93	23.79	32.38	14.66	18.43	972.49	78.9	1051.4
	BF-NM [12] TCSC (6–8)	45.89	57.18	30.77	18.97	15.42	23.69	989.53	59.3	1048.8
	BF-NM [12] TCSC (8–28)	49.98	57.11	30.73	18.99	15.44	23.62	1021.9	27.3	1049.2
	MOPSO (Scenario 3)	38.57	49.73	23.68	45.74	16.85	17.47	992.30	0	992.25
	MOPSO (Scenario 4)	39.78	49.47	24.35	44.08	16.84	16.93	983.36	1.39	984.75

Table 15
The results of the comparison between the proposed method with the method proposed in [12] (the IEEE 118-bus system).

	Fuel cost [$/h]	TCSC cost [$/h]	DR cost [$/h]	Total cost [$/h]
BF-NM [12], without TCSC	72079.3775	0	0	72079.3775
BF-NM [12], with TCSC	71764.8906	15.5974	0	71780.488
MOPSO, with DR	70864.2036	0	151.0206	71015.2242

literature [12]. These findings, considering the congestion limit of 32 MVA for transmission lines, are presented in Table 14.

As shown in this table, using the MOPSO algorithm, the total costs, regardless of the cost of pollution in scenarios 3 and 4, are 579.1814 $/h and 577.8988 $/h, respectively. It should be noted that, in addition to reducing the total cost, generators' production costs have also declined. It is worth noting that in [12] the control method is based on the use of TCSC, while in the present paper, DRP is used.

4.3. IEEE 118-bus test system

In order to assess the performance of the proposed method for larger systems, the obtained results on the IEEE 118-bus system are compared with the method proposed in the literature [12] in Table 15. As it can be observed in the results provided in the table, implementing the proposed method has led to 765.2638 $/h decrease in the total system cost comparing to the method suggested in [12]. It is worth mentioning that the difference depends on the type of the methods proposed and does not necessarily reflect the superiority of the optimization method.

4.4. Evaluation of Pareto set

In literature, several indicators have been presented to evaluate the quality of the solutions obtained from multi-objective optimization methods. For example, in [28], these indicators are classified in the following categories:

- Metrics Assessing the number of Pareto optimal solutions in the set
- Metrics measuring the closeness of the solutions to the True Pareto Front
- Metrics focusing on distribution of the solutions
- Metrics concerning spread of the solutions
- Metrics considering both closeness and diversity

Given that in order to calculate many of these indicators, it should be known that the True Pareto Front categories of indicators are uncountable in our paper. Also, it should be noted that the True Pareto Front is available for mathematical benchmarks [29]. Among the indicators presented in reference [29], the only indicator that is applicable in this paper is the Spacing (*SP*) index.

Table 16
Comparison of the spread metric for MOPSO algorithm (the IEEE 30 bus system).

	The spacing metric (*SP*)
Scenario 1	0.2692
Scenario 2	0.0695
Scenario 3	0.2581
Scenario 4	0.1915
Scenario 5	0.1762

In this section, performance evaluation of the proposed multi-objective algorithm is done by the following criterion.

Spacing metric:

This criterion measures the deviation in the distance between nearest neighbors in terms of Manhattan distance [28,29]. The formulation of this metric is defined as follows:

$$SP = \sqrt{\frac{1}{N-1}\sum_{i=1}^{N}(\bar{d} - d_i)^2} \tag{35}$$

where, N is the number of non-dominated solutions found so far. $\bar{d}$ is the mean of all d_i, $i = 1, \ldots, N$. The parameter d_i is given in following equation.

$$d_i = \min_{\substack{j=1,\ldots,N \\ j \neq i}} (|f_1^i - f_1^j| + |f_2^i - f_2^j|) \tag{36}$$

A value of zero for this metric indicates that all members of the Pareto optimal set are equidistantly spaced. A smaller value of *SP* indicates a better distribution and diversity of the non-dominated solutions.

Table 16 demonstrates the spacing metric (*SP*) of the proposed algorithm in different scenarios.

It should be noted that due to the stochastic nature of the proposed algorithm, a series of 20 independent runs have been carried out.

5. Conclusion and future works

In this paper, the problem of transmission lines congestion management was examined using generation rescheduling and DRPs. The objectives intended in this paper included: minimizing the operating costs, reducing emission, and reducing power system transmission lines congestion. After defining the problem of power system congestion management as a constrained multi-objective optimization problem, multi-objective particle swarm optimization algorithm was used to solve it. Optimization problem was resolved in five different scenarios defined with different control strategies and different transmission lines loadings. The numerical results obtained from these five scenarios on IEEE 30-bus test system were presented in different cases. Results showed that using DRPs increases the operator power of choice in choosing solutions with lower costs and emission levels. In an extreme congestion, considering DRPs in the congestion management studies is inevitable. Moreover, the use of generation rescheduling can somehow meet the power transmission system congestion.

In the future, congestion management shall be used with complex real-world application of various fields such as dynamic congestion management integrated Ramp Rate constraint, probabilistic optimization considering wind or PV systems.

References

[1] N. Amjady, M. Hakimi, Dynamic voltage stability constrained congestion management framework for deregulated electricity markets, Energy Convers. Manage. 58 (2012) 66–75.
[2] J. Romero-Ruiz, J. Pérez-Ruiz, S. Martin, J. Aguado, S. De la Torre, Probabilistic congestion management using EVs in a smart grid with intermittent renewable generation, Electr. Power Syst. Res. 137 (2016) 155–162.
[3] S.A. Hosseini, N. Amjady, M. Shafie-Khah, J.P. Catalão, A new multi-objective solution approach to solve transmission congestion management problem of energy markets, Appl. Energy 165 (2016) 462–471.
[4] F. Ding, J.D. Fuller, Nodal, uniform, or zonal pricing: distribution of economic surplus, IEEE Trans. Power Syst. 20 (2005) 875–882.
[5] J. Han, A. Papavasiliou, Congestion management through topological corrections: a case study of Central Western Europe, Energy Policy 86 (2015) 470–482.
[6] C. Kang, Q. Chen, W. Lin, Y. Hong, Q. Xia, Z. Chen, Y. Wu, J. Xin, Zonal marginal pricing approach based on sequential network partition and congestion contribution identification, Int. J. Electr. Power Energy Syst. 51 (2013) 321–328.
[7] T. Kristiansen, Congestion management, transmission pricing and area price hedging in the Nordic region, Int. J. Electr. Power Energy Syst. 26 (2004) 685–695.
[8] A.K. Jain, S.C. Srivastava, S.N. Singh, L. Srivastava, Bacteria foraging optimization based bidding strategy under transmission congestion, IEEE Syst. J. 9 (2015) 141–151.
[9] M.M. Esfahani, A. Sheikh, O. Mohammed, Adaptive real-time congestion management in smart power systems using a real-time hybrid optimization algorithm, Electr. Power Syst. Res. 150 (2017) 118–128.
[10] S. Verma, V. Mukherjee, Firefly algorithm for congestion management in deregulated environment, Eng. Sci. Technol. Int. J. 19 (2016) 1254–1265.
[11] S. Chellam, S. Kalyani, Power flow tracing based transmission congestion pricing in deregulated power markets, Int. J. Electr. Power Energy Syst. 83 (2016) 570–584.
[12] R.-A. Hooshmand, M.J. Morshed, M. Parastegari, Congestion management by determining optimal location of series FACTS devices using hybrid bacterial foraging and Nelder-Mead algorithm, Appl. Soft Comput. 28 (2015) 57–68.
[13] A. Yousefi, T. Nguyen, H. Zareipour, O. Malik, Congestion management using demand response and FACTS devices, Int. J. Electr. Power Energy Syst. 37 (2012) 78–85.
[14] R. Hemmati, H. Saboori, M. Ahmadi Jirdehi, Stochastic planning and scheduling of energy storage systems for congestion management in electric power systems including renewable energy resources, Energy 133 (2017) 380–387.
[15] S. Verma, V. Mukherjee, Optimal real power rescheduling of generators for congestion management using a novel ant lion optimiser, IET Gener. Transm. Distrib. 10 (2016) 2548–2561.
[16] S.S. Reddy, Multi-objective based congestion management using generation rescheduling and load shedding, IEEE Trans. Power Syst. 32 (2017) 852–863.
[17] S. Gope, A.K. Goswami, P.K. Tiwari, S. Deb, Rescheduling of real power for congestion management with integration of pumped storage hydro unit using firefly algorithm, Int. J. Electr. Power Energy Syst. 83 (2016) 434–442.
[18] C. Li, X. Yu, W. Yu, G. Chen, J. Wang, Efficient computation for sparse load shifting in demand side management, IEEE Trans. Smart Grid 8 (2017) 250–261.
[19] E. Shayesteh, M.P. Moghaddam, A. Yousefi, M.R. Haghifam, M. Sheik-El-Eslami, A demand side approach for congestion management in competitive environment, Int. Trans. Electr. Energy Syst. 20 (2010) 470–490.
[20] A. Tabandeh, A. Abdollahi, M. Rashidinejad, Reliability constrained congestion management with uncertain negawatt demand response firms considering repairable advanced metering infrastructures, Energy 104 (2016) 213–228.
[21] H. Abdi, E. Dehnavi, F. Mohammadi, Dynamic economic dispatch problem integrated with demand response (DEDDR) considering non-linear responsive load models, IEEE Trans. Smart Grid 7 (2016) 2586–2595.
[22] E. Dehnavi, H. Abdi, Determining optimal buses for implementing demand response as an effective congestion management method, IEEE Trans. Power Syst. 32 (2017) 1537–1544.
[23] A. Haque, P. Nguyen, F. Bliek, J. Slootweg, Demand response for real-time congestion management incorporating dynamic thermal overloading cost, Sustain. Energy Grids Netw. 10 (2017) 65–74.
[24] A. Pillay, S.P. Karthikeyan, D. Kothari, Congestion management in power systems – a review, Int. J. Electr. Power Energy Syst. 70 (2015) 83–90.
[25] A. Asadinejad, K. Tomsovic, Optimal use of incentive and price based demand response to reduce costs and price volatility, Electr. Power Syst. Res. 144 (2017) 215–223.
[26] H. Baghaee, M. Mirsalim, G. Gharehpetian, H. Talebi, Reliability/cost-based multi-objective Pareto optimal design of stand-alone wind/PV/FC generation microgrid system, Energy 115 (2016) 1022–1041.
[27] A. Zeinalzadeh, Y. Mohammadi, M.H. Moradi, Optimal multi objective placement and sizing of multiple DGs and shunt capacitor banks simultaneously considering load uncertainty via MOPSO approach, Int. J. Electr. Power Energy Syst. 67 (2015) 336–349.
[28] Gary G. Yen, He Zhenan, Performance metric ensemble for multiobjective evolutionary algorithms, IEEE Trans. Evol. Comput. 18 (2014) 131–144.
[29] David A. Van Veldhuizen, Multiobjective evolutionary algorithms: classifications, analyses, and new innovations (Diss. PhD thesis), in: Presented to the Faculty of the Graduate School of Engineering of The Air Force Institute of Technology, AFIT/DS/ENG, Air University, USA, 1999.